Published online 2 November 2017 *Nucleic Acids Research, 2017, Vol. 45, No. 21* **12585–12598**
doi: 10.1093/nar/gkx1007

*Fn*Cpf1: a novel and efficient genome editing tool for *Saccharomyces cerevisiae*

Michal A. Świat[1], Sofia Dashko[1], Maxime den Ridder[1], Melanie Wijsman[1], John van der Oost[2], Jean-Marc Daran[1] and Pascale Daran-Lapujade[1,*]

[1]Department of Biotechnology, Delft University of Technology, van der Maasweg 9, 2629 HZ Delft, The Netherlands and [2]Laboratory of Microbiology, Wageningen University, Stippeneng 4, 6708 WE Wageningen, The Netherlands

Received July 19, 2017; Revised September 26, 2017; Editorial Decision October 11, 2017; Accepted October 13, 2017

ABSTRACT

Cpf1 is a new class II family of CRISPR-Cas RNA-programmable endonucleases with unique features that make it a very attractive alternative or complement to Cas9 for genome engineering. Using constitutively expressed Cpf1 from *Francisella novicida*, the present study demonstrates that *Fn*Cpf1 can mediate RNA-guided DNA cleavage at targeted genomic loci in the popular model and industrial yeast *Saccharomyces cerevisiae*. *Fn*Cpf1 very efficiently and precisely promoted repair DNA recombination with efficiencies up to 100%. Furthermore, *Fn*Cpf1 was shown to introduce point mutations with high fidelity. While editing multiple loci with Cas9 is hampered by the need for multiple or complex expression constructs, processing itself a customized CRISPR array *Fn*Cpf1 was able to edit four genes simultaneously in yeast with a 100% efficiency. A remarkable observation was the unexpected, strong preference of *Fn*Cpf1 to cleave DNA at target sites harbouring 5′-TTTV-3′ PAM sequences, a motif reported to be favoured by Cpf1 homologs of *Acidaminococcus* and *Lachnospiraceae*. The present study supplies several experimentally tested guidelines for crRNA design, as well as plasmids for *Fn*Cpf1 expression and easy construction of crRNA expression cassettes in *S. cerevisiae*. *Fn*Cpf1 proves to be a powerful addition to *S. cerevisiae* CRISPR toolbox.

INTRODUCTION

CRISPR (Clustered Regularly Interspaced Short Palindromic Repeats) systems are adaptive immune systems widely distributed across bacteria and archaea, designed to destroy DNA of invading mobile genetic elements (1). These immune systems, in which endonucleases are guided by single stranded RNA to find their target DNA, have been turned into powerful genome editing tools over the past few years (2,3). The rapid implementation of CRISPR-based DNA editing systems has tremendously improved molecular toolboxes for a broad spectrum of organisms, ranging from simple prokaryotes to metazoan animals (4). By increasing the speed of genetic engineering, CRISPR-based systems have already impacted the field of microbial biotechnology (5–7). The push towards sustainable alternatives to oil-derived chemicals requires the construction of powerful microbial cell factories that can produce new chemicals, using unnatural substrates at high yields and rates, under harsh industrial conditions. Constructing such advanced cell factories requires extensive and fast genetic engineering strategies, that enable to test various designs in search of the optimal genetic configuration. Even the tractable and genetically accessible model and industrial yeast *Saccharomyces cerevisiae* has rapidly adopted CRISPR-aided DNA editing, making it a standard practice for strain construction (8–10).

Two classes of CRISPR systems have been identified based on the architecture of the CRISPR locus (11–13). Class II, to which the very popular *Streptococcus pyogenes* Cas9 (*Sp*Cas9) belongs, has been favoured for heterologous genome editing mainly due to the structural simplicity of its endonuclease formed of a single subunit (2). Like all CRISPR-based systems, *Sp*Cas9 requires an RNA molecule, called CRISPR-RNA (crRNA) to guide the nuclease towards the editing site (Figure 1). In addition, to target and edit DNA, *Sp*Cas9 requires another RNA fragment, the trans-activating RNA (tracrRNA), that binds to the crRNA and to *Sp*Cas9 (Figure 1). In native systems, the DNA sequences encoding crRNAs (also called spacers) are co-localised in a CRISPR array, in which they are separated by repeated DNA motifs called the Direct Repeats (DRs, Figure 1). In their native system, the repeats of the precursor crRNA transcript base pair with the 'anti-repeat' part of tracrRNA, and these dsRNA helices are recognized and cleaved by RNaseIII (14). For efficient heterologous editing, the CRISPR system is generally simplified by expressing the crRNA already connected to the tracrRNA in a chimeric single guide RNA (sgRNA), and each chimeric

*To whom correspondence should be addressed. Tel: +31 15 278 9965; Email: p.a.s.daran-lapujade@tudelft.nl

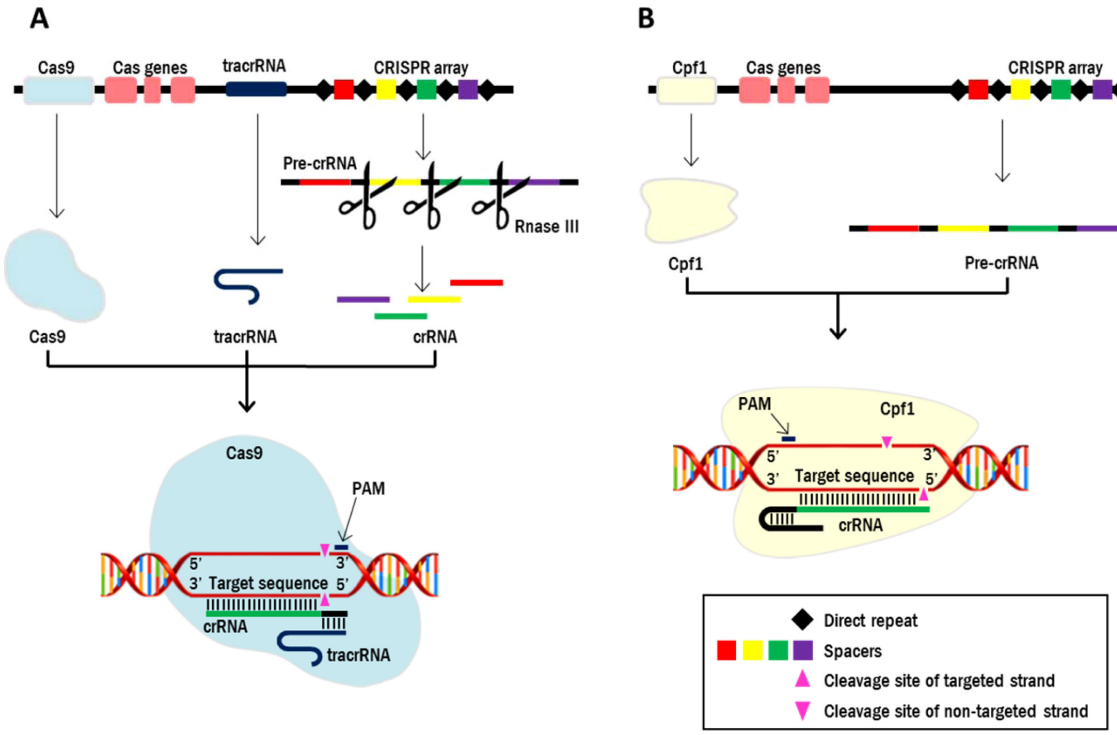

Figure 1. Schematic representation of DNA interference by the Cas9 and Cpf1 endonucleases. As compared to Cas9, Cpf1 does not require a tracrRNA, has a T-rich PAM sequence located at the 5′ end of the protospacer, is capable to mature its own crRNA array, cleaves DNA distal from the PAM and generates staggered ends.

sgRNA is expressed from its own promoter, thereby avoiding the requirement of an RNase for processing the precursor CRISPR-RNA transcript (2) (Figure 1). These sgRNAs have been shown to be functional in a wide variety of organisms, including *S. cerevisiae*, and extensive studies have delivered a number of basic principles to guide the design of crRNAs for efficient *Sp*Cas9-mediated DNA editing (15). However, *Sp*Cas9-based editing has some shortcomings. For instance, as all known CRISPR endonucleases, *Sp*Cas9 can only cut DNA located near a PAM (Protospacer Adjacent Motif) sequence meant to distinguish self from non-self DNA in native immune systems (16–18). The *Sp*Cas9 PAM sequence 5′-NGG-3′ is G-rich and located at the 3′ end of the protospacer (18). While this PAM is rather frequently distributed across the yeast genome (ca. 53 unique genomic targets per 1000 bp, which is the average size of *S. cerevisiae* genes, (8)), it is not always available in the area where editing is desired, more particularly in AT-rich regions. Furthermore, for reasons not yet fully understood, the efficiency of DNA editing varies greatly as a function of the targeted sequence, which further reduces the number of available 'active' PAM sequences. Also, chimeric guide RNAs with individual expression systems are not compatible with multiplex, high-throughput genome editing. The highest number of multisite editing reported so far in yeast is six, but it requires complex plasmid construction for individual expression of each sgRNA and simultaneous transformation of three plasmids, which could be greatly simplified and accelerated using the native CRISPR array systems (9). Non-chimeric gRNAs, based on native CRISPR systems, have been shown to enable *Sp*Cas9-mediated DNA cleavage in *S. cerevisiae*, however their performance for multiplexing is so far an order magnitude lower than that of chimeric systems (19). In *S. cerevisiae*, alternative systems involving ribozymes have been shown to enable dCas9-mediated transcriptional regulation (20), however their efficiency for multisite genome editing has not been explored yet.

Cpf1, a new family of class II CRISPR bacterial endonucleases was recently identified (21) and shown to mediate heterologous DNA editing in bacteria, as well as in plant and mammalian cells (22–27). This enzyme family, recently renamed Cas12a and tentatively classified as Type V-A (12), presents some characteristics reminiscent of Cas9, but also some very distinct and attractive features. Cpf1 variants from three bacteria, *Francisella novicida* (*Fn*Cpf1), *Acidaminococcus* sp. BV3L6 (*As*Cpf1) and *Lachnospiraceae bacterium* (*Lb*Cpf1) have been studied most intensively. Belonging to class II as Cas9, Cpf1 operates as single protein. Resolution of the crystal structure of *Lb*Cpf1 and *As*Cpf1 has shown that Cpf1 and Cas9 share a bi-lobed structure with a central channel in which the RNA-DNA heteroduplex is bound (28–30). However proteins of the Cpf1 family lack HNH domains, and a single RuvC nuclease domain seems to be responsible for cleavage of both DNA strands. In addition they contain a Nuc domain, but current models predict that it is most likely not directly involved in DNA cleavage (30,31). Cpf1 and Cas9 display more striking differences both in structure and function. The Cpf1 PAM is T-rich, and described as 5′-TTTN-3′ (or 5′-TTTV-3′ (32)) for *As*Cpf1 and *Lb*Cpf1, and 5′-TTN-3′ for *Fn*Cpf1, and is

Table 1. List of yeast strains used in this study

Strain name	Genotype	Origin
CEN.PK113–7D	MAT*a MAL2–8c SUC2*	(34)
CEN.PK113–5D	MAT*a ura3–52*	(34)
IMX1139	MAT*a ura3–52 sga1*Δ::*TEF1*p::*Fncpf1::CYC1t::KlURA3*	This study
IME384	MAT*a ura3–52* pUDE731	This study
IME385	MAT*a ura3–52* pUD706	This study
IMX1511	MAT*a ura3–52 sga1*Δ::*TEF1*p::*Fncpf1::CYC1t::KlURA3* Δ*his4* + pUDE713	This study
IMX1512	MAT*a ura3–52 sga1*Δ::*TEF1*p::*Fncpf1::CYC1t::KlURA3* Δ*ade2* Δ*his4* + pUDE709	This study
IMX1522	MAT*a ura3–52 sga1*Δ::*TEF1*p::*Fncpf1::CYC1t::KlURA3* Δ*can1* + pUDE721	This study
IMX1523	MAT*a ura3–52 sga1*Δ::*TEF1*p::*Fncpf1::CYC1t::KlURA3* Δ*can1* + pUDE722	This study
IMX1524	MAT*a ura3–52 sga1*Δ::*TEF1*p::*Fncpf1::CYC1t::KlURA3* Δ*pdr12* + pUDE723	This study
IMX1525	MAT*a ura3–52 sga1*Δ::*TEF1*p::*Fncpf1::CYC1t::KlURA3* Δ*pdr12* + pUDE724	This study
IMX1526	MAT*a ura3–52 sga1*Δ::*TEF1*p::*Fncpf1::CYC1t::KlURA3* Δ*pdr12* + pUDE725	This study
IMX1535	MAT*a ura3–52 sga1*Δ::*TEF1*p::*Fncpf1::CYC1t::KlURA3* Δ*ade2* Δ*can1* Δ*his4* Δ*pdr12* + pUDE735	This study

located at the 5′ end of the protospacer (27). Contrary to Cas9, Cpf1 cleaves DNA distal from the PAM and generates staggered ends (27) (Figure 1). More remarkably, Cpf1 does not require a tracrRNA and is the first known CRISPR endonuclease that harbours a distinct endoribonuclease domain (30,33) (Figure 1). Cpf1 matures the CRISPR-RNA array itself and therefore does not require the activity of an additional RNase (Figure 1). These features propel Cpf1 as an attractive system for multiplex genome editing.

While intensively studied in higher eukaryotes, Cpf1-aided genome editing has been comparatively underexplored in the microbial kingdom. Thus far, Cpf1-mediated DNA cleavage has only been demonstrated in two bacteria, *Escherichia coli* and *Corynebacterium glutamicum* (22,25), and has not been established in lower eukaryotes. The goal of the present study was firstly to evaluate *Fn*Cpf1 functionality for targeted genome editing in *S. cerevisiae*. Secondly, we explored ways to improve the efficiency of genome editing by *Fn*Cpf1 and thereby propose design principles and offer plasmids for efficient DNA cleavage in baker's yeast. Finally, the present work demonstrates that *Fn*Cpf1 can edit multiple genomic loci simultaneously with high efficiency.

MATERIALS AND METHODS

Strains and cultivation techniques

All *S. cerevisiae* strains used in this study belong to the CEN.PK genetic background and are listed in Table 1 (34,35). Yeast cultures were grown in 500 ml shake flasks containing 100 ml of medium at 30°C with 200 rpm agitation. Complex and nonselective media contained 10 g l^{-1} yeast extract, 20 g l^{-1} peptone and 20 g l^{-1} glucose (YPD). When selection was required, YPD was supplemented with 200 mg l^{-1} G418. Synthetic medium containing 3 g l^{-1} KH_2PO_4, 0.5 g l^{-1} $MgSO_4{\cdot}7H_2O$, 5 g l^{-1} $(NH_4)^2SO_4$, 1 ml l^{-1} of a trace element solution, and 1 ml l^{-1} of a vitamin solution as previously described (36) and supplemented with 20 g l^{-1} glucose was used for culture propagation (SMG). When selection on SMG with G418 was required $(NH_4)_2SO_4$ was replaced with 3 g l^{-1} K_2SO_4 and 2.3 g l^{-1} filter-sterilized urea to maintain a stable pH (37). For plasmid propagation, *E. coli* XL1-Blue cells (Agilent Technologies, Santa Clara, CA, USA) were cultivated in Lysogeny broth (LB) medium supplied with ampicillin (100 mg l^{-1}) or kanamycin (50 mg l^{-1}) at 37 °C with 180 rpm agitation. Solid media were obtained by addition of 20 g l^{-1} agar.

Frozen stocks of *S. cerevisiae* and *E. coli* were prepared by addition of the sterile glycerol (30% v/v) to exponentially grown cultures and were stored as frozen aliquots at –80 °C.

Molecular biology techniques

PCR reactions for diagnostic purposes were performed using DreamTaq DNA polymerase (Thermo Fisher Scientific, Walthman, MA, USA) according to manufacturer's instructions. When high fidelity amplification was needed, Phusion® High-Fidelity DNA polymerase (Thermo Fisher Scientific) was used according to supplier's instructions. Oligonucleotides were ordered from Sigma Aldrich (St Louis, MO, USA) with PAGE or desalted purity depending on the purpose. DNA fragments were separated on agarose gels and were excised when purification of the fragment was required (Zymoclean, Zymo Research, Irvine, CA, USA). Bacterial plasmids were isolated using Sigma GenElute Plasmid kit (Sigma-Aldrich). When plasmid purification from yeast was required, Zymoprep Yeast Plasmid Miniprep II Kit was used (Zymo Research). Restriction digestion with DpnI for removal of circular templates (Thermo Fisher Scientific) was performed as recommended in the instruction manual. *E. coli* chemical transformations were performed following manufacturer's recommendations (Agilent Technologies).

Gene deletions were confirmed by diagnostic PCR and Sanger sequencing (Baseclear, Leiden, Netherlands).

Construction of a *S. cerevisiae* strain with genomic integration of *Fncpf1*

The integration construct consisted of two linear DNA fragments, one containing the *Fncpf1* expression cassette and the other harbouring the *KlURA3* marker, which were assembled *in vivo* in yeast and integrated into the *SGA1* locus (Supplementary Figure S1). To construct the *Fncpf1* expression cassette, the human codon-optimized *F. novicida cpf1* tagged with C-terminal nuclear localization signal (NLS) and 3xHA tag was PCR-amplified from pY004 (Addgene plasmid #69976, https://www.addgene.org/69976/, (27)) using primers 10141 and 10144 (Table

Table 2. List of plasmids used in this study

Plasmid	Genotype[a]	Assemby method	Reference
p414-*TEF1*p-*Cas9-CYC1*t	*CEN6/ARS4* amp^R *TRP1TEF1p::Spcas9-CYC1t*		(8)
pMEL10	2 μm amp^R *KlURA3SNR52p*::gRNA-CAN1.Y::*SUP4t*		(9)
pROS13	2 μm amp^R KanMX *SNR52p* ::gRNA-CAN1.Y gRNA-ADE2.Y ::*SUP4t*		(9)
pRS416	*CEN6/ARS4* amp^R *URA3*		(62)
PY004	amp^R *Fncpf1*		(27), Addgene #69976
pUDC175 (Addgene #103019)	*CEN6/ARS4* amp^R *TRP1 TEF1p*::*Fncpf1*::*CYC1t*	*In vivo*	This study
pUD520	KanR *SNR52p::***crADE2–1.L**::*SUP4t*	*GenArt*	This study
pUD521	KanR *SNR52p::***crADE2–2.L**::*SUP4t*	*GenArt*	This study
pUD438	KanR *SNR52p::***crADE2–3.L**::*SUP4t*	*GenArt*	This study
pUD522	KanR *SNR52p*::**crADE2–4.L**::*SUP4t*	*GenArt*	This study
pUD523	KanR *SNR52p*::**crADE2–5.L**::*SUP4t*	*GenArt*	This study
pUD524	KanR *SNR52p*::**crADE2–6.L**::*SUP4t*	*GenArt*	This study
pUD550	KanR *SNR52p*::**crCAN1–1.L***::SUP4t*	*GenArt*	This study
pUD439	KanR *SNR52p::***crCAN1–1.crADE2–3.L**::*SUP4t*	*GenArt*	This study
pUD440	KanR *SNR52p::***crCAN1–1.crHIS4–1.crPDR12–1.crADE2–3.L**::*SUP4t*	*GenArt*	This study
pUD552	KanR *SNR52p*::**crADE2–3.S**::*SUP4t*	*GenArt*	This study
pUD605	2 μm KanMX amp^R *SNR52p::***crADE2–1.L**::*SUP4t*	*In vivo*	This study
pUD606	2 μm KanMX amp^R *SNR52p::***crADE2–2.L**::*SUP4t*	*In vivo*	This study
pUD627	2 μm KanMX amp^R *SNR52p::***crADE2–3.L**::*SUP4t*	*In vivo*	This study
pUD607	2 μm KanMX amp^R *SNR52p*::**crADE2–4.L**::*SUP4t*	*In vivo*	This study
pUD608	2 μm KanMX amp^R *SNR52p*::**crADE2–5.L::***SUP4t*	*In vivo*	This study
pUD609	2 μm KanMX amp^R *SNR52p*::**crADE2–6.L::***SUP4t*	*In vivo*	This study
pUD628 (Addgene #103018)	2 μm KanMX amp^R *SNR52p*::**crADE2–3.S::***SUP4t*	*In vivo*	This study
pUD629	2 μm KanMX amp^R *SNR52p::***crCAN1–1.S***::SUP4t*	*In vivo*	This study
pUD630	2 μm KanMX amp^R *SNR52p::***crCAN1–1.crADE2–3.S**::*SUP4t*	*In vivo*	This study
pUDE712	2 μm KanMX amp^R *SNR52p::***crHIS4–2.S***::SUP4t*	*In vitro*	This study
pUDE713	2 μm KanMX amp^R *SNR52p::***crHIS4–3.S**::*SUP4*t	*In vitro*	This study
pUDE714 (Addgene #103021)	2 μm KanMX amp^R *SNR52p*::**crHIS4–4.S***::SUP4t*	*In vitro*	This study
pUDE708	2 μm KanMX amp^R *SNR52p*::**crADE2–3.crHIS4–2.S**::*SUP4t*	*In vitro*	This study
pUDE709	2 μm KanMX amp^R *SNR52p::***crADE2–3.crHIS4–3.S***::SUP4t*	*In vitro*	This study
pUDE710 (Addgene #103020)	2 μm KanMX amp^R *SNR52p::***crADE2–3.crHIS4–4.S**::*SUP4t*	*In vitro*	This study
pUDE720	2 μm KanMX amp^R *SNR52p*::**crCAN1–2.S***::SUP4t*	*In vitro*	This study
pUDE721	2 μm KanMX amp^R *SNR52p*::**crCAN1–3.S***::SUP4t*	*In vitro*	This study
pUDE722 (Addgene #103022)	2 μm KanMX amp^R *SNR52p*::**crCAN1–4.S***::SUP4t*	*In vitro*	This study
pUDE723	2 μm KanMX amp^R *SNR52p*::**crPDR12–2.S***::SUP4t*	*In vitro*	This study
pUDE724 (Addgene #103023)	2 μm KanMX amp^R *SNR52p*::**crPDR12–3.S***::SUP4t*	*In vitro*	This study
pUDE725	2 μm KanMX amp^R *SNR52p*::**crPDR12–4.S***::SUP4t*	*In vitro*	This study
pUDE735 (Addgene #103024)	2 μm KanMX amp^R *SNR52p*::**crCAN1–4.crHIS4–4.crPDR12–3.crADE2–3.S***::SUP4t*	*In vitro*	This study
pUD706	2 μm amp^R *KlURA3*	*In vivo*	This study
pUDE731 (Addgene #103008)	2 μm amp^R *KlURA3 TEF1p::Fncpf1::CYC1t*	*In vitro*	This study

[a]The presence of an S or a L following the crRNA name indicates that the direct repeats in the CRISPR array are either Short (19 nt) or Long (36 nt), respectively.
The reference number of plasmids deposited to Addgene is indicated next to the plasmid name between brackets when relevant.

2, Supplementary Table S1). The plasmid p414-TEF1p-cas9-CYC1t (Addgene plasmid #43802) backbone was amplified with primers 10145 and 10146. The amplified *Fncpf1* and p414-TEF1p-cas9-CYC1t fragments were assembled using NEBuilder® HiFi DNA Assembly Master Mix (New England BioLabs, Ipswich, MA, USA) resulting in plasmid pUDC175 (Table 2). The newly constructed $TEF1_p$::*Fncpf1*::$CYC1_t$ expression unit was amplified from pUDC175 with Phusion® High-Fidelity DNA Polymerase (ThermoFischer Scientific) and primers 10147 and 10189 (Supplementary Table S1) which introduced a short homology to the *SGA1* chromosomal locus and an homology the co-transformed fragment respectively. The *KlURA3* integration fragment was PCR-amplified with Phusion® High-Fidelity DNA Polymerase (ThermoFischer Scientific) using primers 10190 and 10192 which introduced an homology to the *Fncpf1* fragment and an homology to the chromosomal *SGA1* locus respectively, and using pMEL10 as template (Table 2, Supplementary Table S1). Two micrograms of each integration fragment were transformed to *S. cerevisiae* CEN.PK113–5D (*MAT*a *ura*3–52, Table 1) using the lithium acetate transformation protocol (38). Transformants were selected on SMG plates. Correct assembly and integration of the cassette in the *SGA1* locus were verified via PCR with primers listed in Supplementary Table S1. After a second restreaking, a single colony isolate was selected, named IMX1139 (Table 1), and its genome was sequenced.

Construction of a *S. cerevisiae* strain expressing *Fn*Cpf1 from a multicopy plasmid

A multicopy plasmid encoding *Fncpf1* was constructed by Gibson assembly of the pMEL10 backbone, obtained by amplification of pMEL10 using primers 2055 and 4173 (Supplementary Table S1), and the *Fncpf1* expression cassette (amplified with primers 5976 and 2629 using pUDC175 as a template (Supplementary Table S1)). Plasmid assembly was confirmed by PCR analysis using primers 2376 and 10408 (Supplementary Table S1) and restriction digestion analysis using FastDigest PdmI (Thermo Fisher Scientific). The resulting plasmid was named pUDE731 (Table 2). 500 ng of pUDE731 were transformed to CEN.PK113–5D (*MAT*a *ura*3–52, Table 1) using the lithium acetate transformation protocol (38). To obtain an empty plasmid used as control for pUDE731, PCR-amplified pMEL10 backbone (primers 2055/4173) and repair oligo made with primers 12269/12270 were cotransformed into CEN.PK113–5D for *in vivo* assembly. Transformants containing pUDE731 and the *in vivo* assembled empty plasmid were selected on SMG plates and checked using diagnostic PCR with primers 2376 and 10408 on genomic DNA prepared as previously described (39). A clone carrying pUDE731 and showing the expected bands was additionally confirmed by Sanger sequencing of a DNA fragment containing the *Fncpf1* expression cassette, amplified using primers 2750/2376 and 4661 (Supplementary Table S1). This strain was named IME384 (Table 1). A transformant shown to carry the empty plasmid by PCR was further characterized by restriction analysis. The strain was named IME385 (Table 1) and the verified empty plasmid pUD706 (Table 2).

Selection of target sites, design of crRNA arrays

In first instance, to knock-out the targeted genes (*ADE2, HIS4, PDR12* and *CAN1*) spacers were designed following several criteria: (i) both strands of the coding region of the target genes were screened for the presence of a PAM of 5′-TTN-3′. For every PAM found, 25nt downstream were selected as potential target sequence; (ii) sequences containing poly-T stretches longer than six were discarded due to the possibility of premature RNA polymerase III transcripts formation (8,40); (iii) spacers exhibiting similarity with other chromosomal loci determined by the BLASTn webtool (41) were considered as possible off-targets and were excluded; iv) target sequences fulfilling the three first criteria were screened for their AT content and secondary structure of the mature crRNA. The crRNA structure was analysed using the RNA fold web server (42), only open RNA secondary structures were favoured, as they might allow efficient interaction with *Fn*Cpf1.

As several spacers designed with these criteria did not promote efficient *Fn*Cpf1-mediated DNA editing, new design principles were defined and tested as described in the Results section.

Construction of crRNA expression plasmids

The crRNA expression cassettes systematically comprised the RNA polymerase III dependent *SNR52* promoter, the target sequence(s) flanked by direct repeats and the *SUP4* terminator. crRNA arrays were either ordered as linear synthetic fragments (IDT-BVBA, Leuven, Belgium) and directly assembled into a plasmid backbone, or synthetized by GenArt on plasmids (Regensburg, Germany) with further assembly. Two types of direct repeats were tested, a long repeat of 36 nt (GTCTAAGAACTTTAAATAATTTCTACTGTTGTAGAT) and a short repeat of 19 nt (AATTTCTACTGTTGTAGAT).

crRNA expression constructs were obtained using two different methods. crRNA expression plasmids were initially constructed by *in vivo* assembly of four fragments (Table 2) (43). For this purpose, a mixture containing a DNA fragment with the amp^R marker, a 2 micron fragment for yeast propagation, a KanMX marker cassette and the synthetized linear crRNA array was transformed in IMX1139. Each fragment was PCR-amplified using template plasmids pRS416 for amp^R, pROS13 for 2μm and kanMX, with primers pairs 2054/2055, 10224/10225, 10313/10314, respectively (Supplementary Table S1). These primers incorporated orthogonal sequences (Synthetic Homologous Recombination sequences, SHR, (43)) to each fragment, thereby enabling their assembly by homologous recombination in yeast. Primer pair 10477/10478 was used to amplify the crRNA arrays from a corresponding plasmid synthetized by GeneArt (Table 2), while incorporating SHR's (Supplementary Table S1). Fragments were digested by DpnI (Thermo Fisher Scientific) and gel-purified prior to transformation. For transformation 100 fmol of 2μm and KanMX fragments and 200 fmol of crRNA fragment and amp^R were supplied (44). The plasmids constructed using this method were named pUD605 to pUD609 and pUD627 to pUD630 (Table 2).

To evaluate the effect on DNA delivery on *Fn*Cpf1 efficiency, crRNA plasmids pUD627 and pUD628 (Table 2) constructed by *in vivo* assembly were extracted from *S. cerevisiae* transformants. The extracted plasmids were checked by restriction analysis using FD PstI and FD PvuI. Additionally, the spacer region was Sanger sequenced with the primer pair 10477/10478. For transformation, 500 ng of the corresponding plasmid was transformed in IMX1139.

A second set of plasmids was assembled *in vitro* using NEBuilder® HiFi DNA Assembly Master Mix (New England Biolabs) targeting either a single locus *HIS4* (crHIS4–2, crHIS4–3 and crHIS4–4), *ADE2* (crADE2–3), *CAN1* (crCAN1–2, crCAN1–3, crCAN1–4), *PDR12* (crPDR12–2, crPDR12–3, crPDR12–4) or targeting multiple loci (crADE2–3.crHIS4–2, crADE2–3.crHIS4–3, crADE2–3.crHIS4–4, and crCAN1–4.crHIS4–4 .crPDR12–3.crADE2–3). To this end, a linear fragment with crRNA array was assembled with a PCR-amplified fragment of pUD628 (primers 5793 and 11940). crRNA array and plasmid backbone harboured 60 nt homology flanks to promote assembly of the two fragments. Correct plasmid assembly was confirmed by diagnostic PCR and Sanger sequencing. The plasmids were named pUDE708 to pUDE714, pUDE720 to pUDE725 and pUDE735 (Table 2). For transformation to IMX1139, 500 ng of plasmid DNA were used, with the exception of the transformations presented in Figure 7 for which 2 μg were used. pUD628 (Addgene #103018), pUDE714 (Addgene #103021),

pUDE722 (Addgene #103022) and pUDE724 (Addgene #103023) carrying crADE2–3, crHIS4–4, crCAN1–4 and crPDR12–3, respectively for single deletion, pUDE710 (Addgene #103020) carrying crADE2–3 and crHIS4–4 for double deletion, and pUDE735 (Addgene #103024) carrying the quadruple arrays combining crCAN1–4, crHIS4–4, crPDR12–3 and crADE2–3 are available from Addgene (Table 2). These plasmids carry crRNAs framed by short DRs of 19 nt. Also, pUDC175 (Addgene #103019) and pUDE731 (Addgene #103008), centromeric and episomal plasmids respectively, harbouring *Fncpf1* for expression in *S. cerevisiae*, are available from Addgene (Table 2).

Strain construction through *Fn*Cpf1-mediated genome editing

The crRNA array expression plasmids or plasmid fragments were transformed to IMX1139 or IME384 expressing *Fn*Cpf1. 1 μg of 120 bp dsDNA repair DNA was co-transformed to enable repair of the edited genomic locus by homologous recombination. As exception, 2 μg of repair DNA were co-transformed in the experiments shown in Figure 7. To assess crRNA efficiency an identical transformation omitting the repair DNA fragment was systematically performed. The repair DNA fragment was generated by annealing in a 1:1 ratio two complementary 120 nt oligonucleotides that were initially heated at 95°C and then cooled down to room temperature (9). Transformed cells were plated on solid YPD plates supplemented with G418. In the case of IME384, transformants were selected on SMG with G418 and urea as a nitrogen source, supplemented with 20 mg l^{-1} adenine and 125 mg l^{-1} of histidine. When extended incubation was tested, 100 μl of the transformed cells were first recovered on YPD for 24–48 h before plating. Duplicate transformations were performed for each experiment and dilutions of 10^{-1}, 10^{-2} and 10^{-3} were plated.

Whole genome sequencing

The genome of IMX1139 was sequenced using MiSeq (Illumina, San Diego, CA, USA) with MiSeq® Reagent Kit v3 with 2 × 300 bp read length. Genomic DNA was extracted using the Genomic DNA kit (Qiagen, Hilden, Germany). Extracted DNA was quantified by BR ds DNA kit using Qubit spectrophotometer (Invitrogen, Carlsbad, CA, USA) and mechanically sheared with the M220 ultrasonicator (Covaris, Woburn, MA, USA) using settings aiming at 550 bp average size. DNA libraries were prepared using the TruSeq DNA PCR-Free Library Preparation Kit according to the manufacturer's instructions (Illumina). qPCR quantification of libraries was done with the KAPA Library Quantification Kit for Illumina platforms (Kapa Biosystems, Wilmington, MA, USA) on a Rotor-Gene Q PCR cycler (Qiagen). Sequence reads of genomic DNA were mapped onto the CEN.PK113–7D reference strain sequence (35) and on the unique integrated *Fncpf1-KlURA3* contig using the Burrows–Wheeler Alignment tool (BWA) and further processed using SAMtools (45,46). The sequencing raw data are available at NCBI (https://www.ncbi.nlm.nih.gov/bioproject/) under the Bioproject number PRJNA394199.

Growth rate measurements

To evaluate the potential toxicity of *Fn*Cpf1 expression in *S. cerevisiae*, IMX1139 (expressing *Fncpf1* from a chromosomal locus), IME384 (expressing *Fncpf1* from a multicopy plasmid pUDE731), IME385 (containing the empty multicopy plasmid pUD706) and CEN.PK113–7D (Table 1) were grown in SMG medium in shake-flask culture. Growth was monitored by measuring optical density (660 nm) at regular time intervals using Libra S11 spectrophotometer (Biochrom, Cambridge, UK). The maximum specific growth rates were calculated from duplicate shake-flask cultures.

RESULTS

*Fn*Cpf1 expression from genomic DNA is not toxic for *S. cerevisiae*

*Fn*Cpf1-mediated genome editing in *S. cerevisiae* requires three parts, (i) the endonuclease Cpf1, (ii) the crRNA that will guide Cpf1 to the targeted DNA site, and (iii) a small, double stranded DNA fragment that will elicit repair of the double strand DNA cleavage caused by *Fn*Cpf1 via homologous recombination and thereby restore chromosome integrity (repair DNA). A yeast strain carrying a single copy of the *Fncpf1* gene from *Francisella novicida* U112 integrated in its genome was therefore constructed (Supplementary Figure S1). A *Fncpf1* allele that was codon-optimized for expression in human and fused at its C-terminus with the nuclear localization signal (27) was cloned between the strong and constitutive *TEF1* promoter and the *CYC1* terminator. Together with the *URA3* gene from *Kluyveromyces lactis*, the *Fncpf1* expression cassette was integrated in the *SGA1* locus on chromosome IX of *S. cerevisiae* strain CEN.PK113–5D. PCR analysis and whole genome sequencing of a selected transformant, renamed IMX1139, confirmed the correct integration, copy number and sequence for *Fncpf1* (Supplementary Figure S1). Moreover, whole genome sequencing also revealed the absence of unwanted mutations or chromosomal rearrangements in IMX1139.

The impact of *Fncpf1* and its translation product on growth of *S. cerevisiae* was assessed. The prototrophic IMX1139 grew as fast as the isogenic control strain CEN.PK113–7D in chemically defined medium with glucose as sole carbon source at 30°C (specific growth rate of 0.41 ± 0.01 h^{-1} and 0.42 ± 0.01 h^{-1} for IMX1139 and CEN.PK113–7D, respectively), revealing that *Fn*Cpf1 expression had no detectable impact on *S. cerevisiae* physiology (Figure 2A).

To further explore the potential toxicity of *Fn*Cpf1, a strain expressing *Fn*Cpf1 from a multicopy plasmid, using the same strong, constitutive promoter as the one used for IMX1139, was constructed. When grown in shake-flask, this strain, IME384, displayed a substantial decrease in specific growth rate (24% decrease). IME384 grew at 0.29 ± 0.00 h^{-1} while its isogenic control strain IME385 (carrying the corresponding empty plasmid) grew at a specific growth rate of 0.38 ± 0.00 h^{-1} (Figure 2B), demonstrating the toxicity of *Fn*Cpf1 at extreme expression levels.

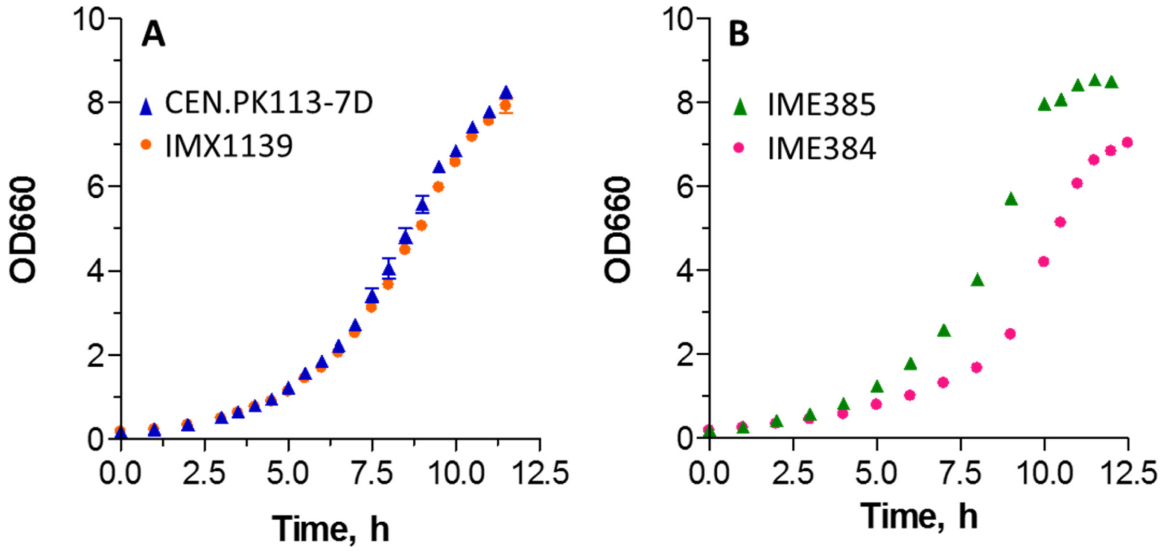

Figure 2. Specific growth rate of strains expressing *Fn*Cpf1 and their control strains. A: IMX1139, expressing *Fn*Cpf1 constitutively from its genomic DNA, and its congenic control strain CEN.PK113–7D. B: IME384, expressing *Fn*Cpf1 from a multicopy plasmid (pUDE731) and its congenic control strain IME385 containing the same multicopy plasmid but without *Fn*Cpf1 (pUD706). The strains were cultivated in shake-flask on chemically defined medium with glucose as sole carbon source. The data points represent the average and mean deviation of two independent culture replicates.

*Fn*Cpf1 is capable of RNA-mediated targeted genomic DNA editing in *S. cerevisiae*

To supply the crRNA to IMX1139 and promote *Fn*Cpf1-mediated DNA cleavage, crRNA expression cassettes carrying the constitutive *SNR52* promoter, a single 25-nt spacer surrounded by two direct repeats of 36 nt from *Francisella novicida* (27) and the *SUP4* terminator were synthetized (Figure 3A). To easily monitor *Fn*Cpf1 activity, the spacer was designed to target *ADE2*, a gene essential for adenine biosynthesis, deletion of which results in adenine auxotrophy and in red colouring of colonies (47). The 5′-TTN-3′ PAM previously defined for *Fn*Cpf1 (27) was used to select the targeted DNA sequence. The plasmid carrying this crRNA expression cassette was assembled in yeast using *in vivo* assembly (43), (Figure 3A) by transforming the following four fragments to yeast: (i) the crRNA expression cassette, (ii) a yeast selection marker, (iii) a yeast autonomous origin of replication and (iv) a selection marker together with origin of replication for expression in *E. coli*. These four fragments of the CRISPR plasmid were transformed to yeast together with the DNA fragment (i.e. repair DNA) meant to promote repair of the chromosomal cleavage caused by *Fn*Cpf1.

While various software algorithms are available to guide crRNA design for *Sp*Cas9 in *S. cerevisiae* (9,48–50) for maximal cleavage efficiency and specificity, design principles for the newly discovered *Fn*Cpf1 are still being explored. Both the AT content of the gRNA and the site of cleavage are important for efficient genome editing by *Sp*Cas9 (51). Therefore, six crRNA with AT contents ranging from 36% to 84% and targeting sequences spread across the whole coding sequence of *ADE2* were chosen (crADE2–1 to crADE2–6, Figure 3B, Table 3 and Supplementary Table S2). PCR analysis of the cleavage site confirmed that DNA was cleaved as expected and correctly repaired via homologous recombination by the supplied repair DNA fragment (Figure 3C and Supplementary Figure S2). The six crRNAs led to very different editing efficiencies ranging from below 1% to 37%. However, similar efficiencies were obtained for AT contents ranging from 36 to 72% (28 ± 2% and 29 ± 4% respectively), revealing that *Fn*Cpf1 was not sensitive to large variations in AT content within this range. While the 84% AT content could explain why the efficiency of this crADE2–6 was very low, also crADE2–2 and crADE2–4 with 44% and 60% AT content hardly led to genome editing. These results suggested that other factors than AT content did affect the *Fn*Cpf1 endonuclease activity.

To increase the editing efficiency that was overall relatively low, cells were incubated after transformation in liquid medium for 48 hours. This incubation did successfully increase the editing efficiency up to 78 ± 4% for the three crRNAs that gave the highest efficiencies right after transformation (crADE2–1, crADE2–3 and crADE2–5), but did not improve the efficiency for the other three crRNAs (Figure 3C). As the double-stranded repair DNA supplied to cells is rapidly degraded by nucleases in the hours following transformation, new DNA cuts resulting from *Fn*Cpf1 activity during prolonged incubation of cells in liquid medium can only result in repair via non-homologous end joining (NHEJ). However, PCR analysis and sequencing of ten colonies with the red phenotype after 48 hours incubation revealed that the DNA cleavage caused by *Fn*Cpf1 was exclusively repaired by integration of the supplied repair DNA via homologous recombination (Supplementary Figure S2). During prolonged incubation, in the absence of repair DNA and due to the low occurrence of DNA repair by NHEJ in *S. cerevisiae*, failure to repair the double strand DNA cleavage caused by *Fn*Cpf1 results in cell death. The surviving cells, *i.e.* cells that have already performed *ADE2* editing and repair by homologous recombination shortly after transformation, appeared to be enriched in the culture.

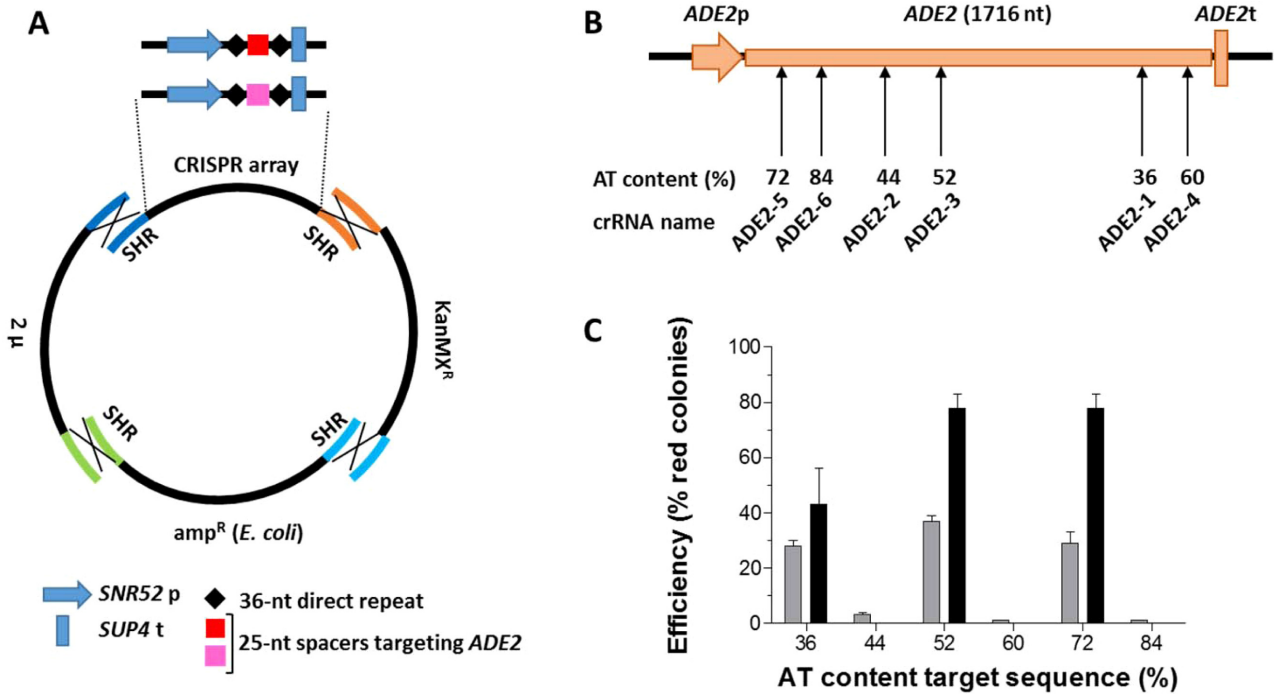

Figure 3. Efficiency of *ADE2* editing by *Fn*Cpf1. (**A**) Design of the CRISPR plasmid harbouring the CRISPR array for *in vivo* assembly in yeast. SHR, homologous sequence for recombination (43). (**B**) AT content and position in the coding region of *ADE2* of the crRNAs. (**C**) Comparison of the genome editing efficiency of six crRNA with various AT content and target sequence (grey bars). The genome editing efficiency was also measured when cells were incubated after transformation in liquid medium for 48 h (black bars). The efficiency is calculated as the number of red colonies divided by the total number of colonies on the transformation plates in the presence of repair DNA fragments. Values represent the average and standard deviation of two biological and two technical replicates. (Plasmids used: pUD605 to pUD609, Table 2).

Table 3. Attributes of the spacers used in this study

Targeted gene	crRNA name	5′ to 3′ sequence **(PAM)**	AT content (%)	Position from ATG
ADE2 (1716 nt)	crADE2–1	T**(TTA)**CGGGCACACCGATGACAGGAAGTGG	36	1438
	crADE2–2	T**(TTT)**CGGCGTACAAAGGACGATCCTTCAG	44	723
	crADE2–3	T**(TTC)**CCGGTTGTGGTATATTTGGTGTGGA	52	743
	crADE2–4	T**(TTA)**CATTCAATTGTGCAAATGCCTAGAG	60	1498
	crADE2–5	T**(TTA)**ATTTGGGATGTTTTACTTGAAGATT	72	247
	crADE2–6	T**(TTG)**ATTAAATGCTCTTTTTGAATATATT	84	317
CAN1 (1773 nt)	crCAN1–1	T**(TTA)**TTTGGTCTATCAAAGAACAAGTTGG	64	1204
	crCAN1–2	CTT**(TTC)**ATTGGTTTATCCACACCTCTGACCA	64	322
	crCAN1–3	CAT**(TTC)**AAGGTACTGAACTAGTTGGTATCAC	60	893
	crCAN1–4	GTT**(TTG)**CCACATATCTTCAACGCTGTTATCT	60	1123
HIS4 (2400 nt)	crHIS4–1	G**(TTG)**CCCAATGTAAGGAGATTGTGTTTGC	56	1514
	crHIS4–2	T**(TTC)**TCCAATCAATTCATGGTAAAACAAA	72	328
	crHIS4–3	T**(TTA)**CTAAAGATTCTAGCCCCACCAAACC	52	730
	crHIS4–4	T**(TTA)**GCATCTTGGCTAGCAATGAACAGAG	52	227
PDR12 (4536 nt)	crPDR12–1	A**(TTC)**CATTTATGAAATATGAAGCTGGTGC	64	1847
	crPDR12–2	CAT**(TTC)**GTCGAGATCGAACCATGACGATGAT	52	39
	crPDR12–3	GTT**(TTA)**GCACAAAGAATCAATATGGGTGTCA	60	2674
	crPDR12–4	CAT**(TTC)**GCATATAAGCATGCTTGGAGAAATT	62	2269

NB: in the text and in Table 2, a letter is added at the end of the crRNA name listed in this table to indicate whether the crRNA is framed by short (S, 19 nt) or long (L, 36 nt) direct repeats.

Direct repeat length has a strong impact on *Fn*Cpf1-mediated genome editing in *S. cerevisiae*

It has been shown in several hosts that shorter DR can improve efficiency of genome editing by *Fn*Cpf1 (52). New CRISPR cassettes were synthetized with DR of 19 nt instead of the 36 nt previously used, framing the crADE2–3 spacer targeting *ADE2* (crADE2–3.S, in which the letter S after the crRNA name denotes short DRs in contrast with L that denotes a long DRs (36 nt)). Shortening the DR length had a marked impact on editing efficiency as transformation plates were covered with red colonies, and white colonies were virtually absent, leading to knockout efficiencies of 100% (Table 4). In addition, transformation with CRISPR cassettes with 36-nt DR typically led to

Table 4. *ADE2* editing efficiency of *Fn*Cpf1 for interruption and point mutation using long (36 nt) and short (19 nt) direct repeats

Protospacer	DR length	Mutation type	Plasmid assembly[a]	Genome editing efficiency
crADE2–3 (52% AT)	36 nt	Deletion	*in vivo*	37 ± 2%[b]
	36 nt	Deletion	Pre-assembled	19 ± 6%[b]
	19 nt	Deletion	Pre-assembled	100%[2]
	19 nt	Point mutation	Pre-assembled	100%[c]

[a]Pre-assembled plasmids were purified from yeast cells after *in vivo* assembly and re-used for transformation to yeast.
[b] Efficiency calculated as the number of red colonies divided by the total number of colonies on the transformation plates in the presence of repair DNA fragments. Values represent the average and standard deviation of two biological and two technical replicates.
[c] Efficiency calculated by dividing the number of colonies with the correct point mutation over the total number of colonies tested.

the formation of a substantial number of white colonies in the absence of repair DNA (typically 30–40 colonies per 100 colonies counted in the presence of repair DNA in experiments presented in Figure 3). In these colonies the selection marker was present, but *Fn*Cpf1 was not able to cleave DNA. When using CRISPR cassettes with 19-nt DR, hardly any colonies were observed when repair DNA was omitted from the transformation mix.

For experiments with shorter direct repeats, CRISPR plasmids were first pre-assembled by *in vivo* assembly, then purified from the yeast strains before being transformed to cells in which the genome editing efficiency was monitored. Conversely, genome editing efficiency in experiments shown in Figure 3 was tested directly in cell populations in which the CRISPR plasmids were directly assembled *in vivo*. To check whether the aforementioned improved efficiency resulted from utilization of pre-assembled plasmid and not from shorter DR, we repeated *ADE2* editing with crADE2–3.L using 36 nt direct repeats, but this time with a pre-assembled CRISPR plasmid. Efficiency was not improved, and even slightly decreased using pre-assembled plasmids, confirming that shorter direct repeats were responsible for the strongly enhanced *Fn*Cpf1-mediated genome editing (Table 4).

*Fn*Cpf1 is an efficient tool to insert point mutations

To take genome editing one step further, *Fn*Cpf1 was assessed for *in vivo* site directed mutagenesis in *S. cerevisiae*. A 120 nt repair fragment was designed, carrying a two nucleotide change to mutate the PAM and incorporate a premature TAA stop codon in the middle of *ADE2* coding sequence, thereby leading to a shortened *ADE2* transcript and hence an inactive phosphoribosylaminoimidazole carboxylase. Mutation of the PAM aimed at preventing further cleavage of *ADE2* by *Fn*Cpf1. The red colour of the obtained colonies indicated that the transformants were effectively targeted and sequencing of the *ADE2* locus confirmed the integration of the premature stop codon in the PAM in all tested transformants (Table 4 and Figure 4). *Fn*Cpf1-mediated genome editing therefore very efficiently generated point mutations at a user-specified location in the genome of *S. cerevisiae*.

Efficient simultaneous editing of two genomic targets by *Fn*Cpf1

To test double and quadruple deletion, CRISPR arrays targeting *ADE2* and *CAN1* or *ADE2*, *CAN1*, *HIS4* and *PDR12* were synthetized (Supplementary Figure S3). All spacers had similar AT content ranging from 52% to 64% (Table 3). The crRNA targeting *ADE2* was systematically located at the last position of the array before the terminator and long repeats (36 nt) were used. Unexpectedly, no *Fn*Cpf1-mediated deletion was observed for *CAN1* either using single, double or quadruple CRISPR array (Supplementary Figure S3). Similarly, diagnostic PCR revealed that neither *HIS4* nor *PDR12* were deleted when using the quadruple CRISPR array (Supplementary Figure S3). PCR analysis would fail to identify *Fn*Cpf1 editing if the cleavage was not repaired via homologous recombination but rather by non-homologous end joining, as the latter would lead to short indels that can only be identified by sequence analysis. However, none of the sequenced transformants (20 transformants from the plates with repair DNA and 10 from the plates without repair for each targeted gene) carried indels at the targeted locus, revealing that crCAN1.L, crHIS4–1.L and crPDR12.L failed to induce *Fn*Cpf1-mediated genome editing (Supplementary Figure S4). This lack of DNA editing by *Fn*Cpf1 was confirmed at a larger scale by phenotypic analysis of transformants. Remarkably, however, *ADE2* was successfully deleted whether the crRNA was carried by the single, double or quadruple crRNA array (Supplementary Figure S3). Moreover, the efficiency of *ADE2* deletion was not substantially reduced when four loci (28 ± 4% efficiency) were targeted as compared to single locus targeting (36 ± 2% efficiency; Supplementary Figure S3).

As several crRNAs failed to promote *Fn*Cpf1-mediated gene deletion, we designed a series of three crRNAs targeting the *HIS4* gene (Table 3). These three new crRNAs named crHIS4–2, crHIS4–3 and crHIS4–4 were tested for single deletion, as well as for double deletion, in combination with crADE2–3.S (Figure 5A). For this experiment, short direct repeats of 19 nucleotides were used, and the plasmids carrying the crRNAs were assembled *in vitro*, prior to transformation. Deletion was checked by diagnostic PCR (Supplementary Figure S5). As shown in the previous experiments, crADE2–3.S led to very efficient *Fn*Cpf1-mediated editing of *ADE2* when using a single target, but remarkably, when targeting both *ADE2* and *HIS4*, crADE2–3.S also promoted *ADE2* deletion with 100% efficiency with any of the crRNAs targeting *HIS4* (Figure 5B). crHIS4–2.S, crHIS4–3.S and crHIS4–4.S displayed different editing efficiencies for single locus targeting, with HIS4–2.S being unable to guide *Fn*Cpf1 for editing, while the latter two crRNAs resulted in *HIS4* deletion with 86% and 100% efficiency, respectively. When combined with crADE2–3.S

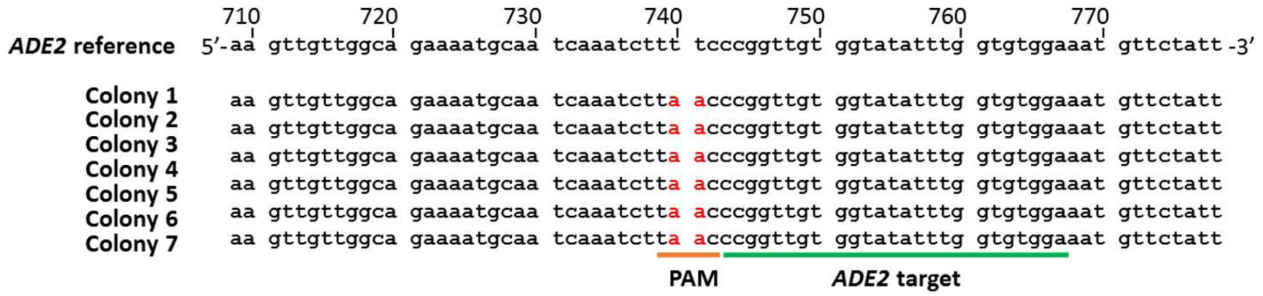

Figure 4. Confirmation of *Fn*Cpf1-mediated introduction of a point mutation in *ADE2*. Sanger sequencing of the genomic DNA locus targeted for *Fn*Cpf1-mediated point mutation in seven randomly selected transformants. The control is the genomic DNA of the congenic strain CEN.PK113–7D. (Plasmid used: pUD628 carrying crADE2–3.S, Table 2).

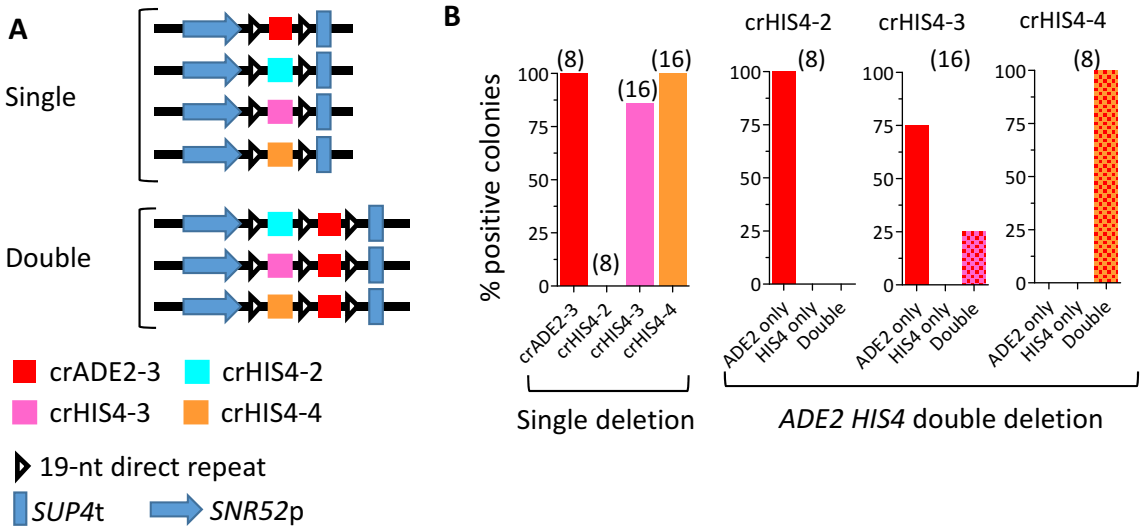

Figure 5. *Fn*Cpf1-mediated editing of single and double genomic targets. (**A**) Composition of CRISPR arrays for single and double deletion of *ADE2* and *HIS4*. 19-nt direct repeats were used and CRISPR plasmids were assembled *in vitro* using Gibson assembly. (**B**) Fraction of transformants with single or double deletion as measured by diagnostic PCR (Supplementary Figure S5), following the design described in A. The number of transformants checked by PCR is indicated between brackets. (Plasmids used: pUD628, pUDE712 to pUDE714, pUDE708 to pUDE710). Plating was performed just after transformation, without additional incubation.

for double targeting, crHIS4–2.S failed to promote gene deletion, while 25% of the tested clones displayed double deletion when using crHIS4–3.S (Figure 5B). 100% of the tested transformants displayed a double *ADE2 HIS4* deletion when using crADE2–3.S and crHIS4–4.S, without requirement of extended incubation, thereby demonstrating that *Fn*Cpf1 does have the potential to very efficiently promote multisite homologous recombination-mediated DNA editing.

Refining the guidelines for crRNA design for predictable and efficient multiplex genome editing up to four targets in *S. cerevisiae*

Remarkably, seven out of the twelve tested crRNA guides resulted in no or extremely low (below 3%) genome editing efficiencies. For these crRNAs, sequence analysis of the targeted sites revealed the complete absence of DNA editing by *Fn*Cpf1. Comparing the PAM of these crRNAs strikingly revealed that the PAM of efficient crRNAs shared characteristics that have been shown to strongly enhance DNA editing efficiency with Cpf1 from *Acidaminococcus* (*As*Cpf1) and *Lachnospiraceae* bacterium (*Lb*Cpf1) (26,27,31). These two Cpf1 variants favour a 5′-TTTV-3′ PAM (V = A/G/C), which differs from the reported *Fn*Cpf1 PAM (5′-NTTN-3′) by a strong preference for a thymidine at the 5′ position of the PAM, and by a marked decrease in efficiency in the presence of thymidine at the 3′ end (31). The same study revealed that thymidine is strongly disfavoured in the first position after the PAM. Remarkably, out of the six crRNAs with AT content within acceptable range (44–72%) that failed to promote genome editing in *S. cerevisiae*, five do not meet the criteria defined for *As*Cpf1 and *Lb*Cpf1 (Figure 6). Two have a thymidine in the first position after the PAM (TTTA-**T**, crCAN1; TTTC-**T**, crHIS4–2), two do not harbor thymidine in the 1st position of the PAM (**G**TTG-C, crHIS4–1; **A**TTC-C, crPDR12) and one has a thymidine in the last position of the PAM (TTT**T**-C, crADE2–2). These results suggested that *Fn*Cpf1 preferred 3′-TTTV-5′ as PAM, and the absence of thymidine as first base after the PAM, when expressed in *S. cerevisiae*. We used these new criteria to design crRNAs targeting *CAN1* and *PDR12*. Out of the six new crRNAs, five were

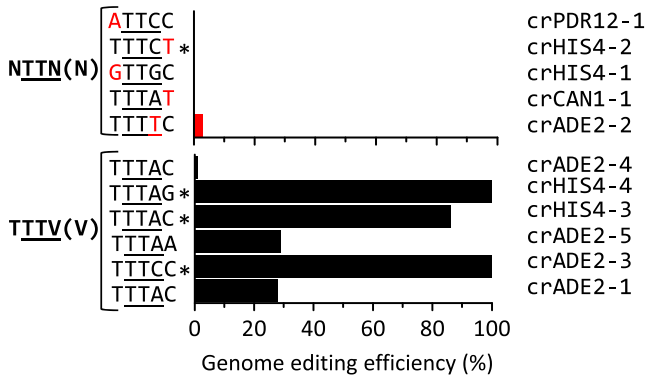

Figure 6. Overview of PAM sequences of the crRNAs used in this study and their efficiency for genome editing. Only crADE2–6, which had an extreme AT content (84%) is not represented. Efficiency calculated as indicated in Figures 3 and 5. * indicates arrays containing 19-nt repeats instead of 36.

able to promote *Fn*Cpf1-mediated genome editing (Figure 7), demonstrating that the new design criteria increased the predictability of genome editing by *Fn*Cpf1.

As crRNAs able to efficiently target four different loci in yeast genomic DNA were available, we explored their ability to target these four loci simultaneously. An array carrying crCAN1–4, crHIS4–4, crPDR12–3 and crADE2–3 was synthetized (with short DR, pUDE735) and transformed to IMX1139 (carrying a chromosomal copy of *Fncpf1*), as well as to IME384, a strain expressing *Fn*Cpf1 from a multicopy vector (Figure 7). Both strains showed an extremely high level of quadruple deletion, as 88% and 100% of the tested cloned displayed four simultaneous deletions in IMX1139 and IME384 respectively (Figure 7, Supplementary Figure S6). Remarkably, the efficiency of DNA editing was not affected by positioning of the crRNA on the array as the deletion efficiency of *ADE2* was 100% in all tested arrays, and all four targets were equally well edited. It is noteworthy that the number of colonies obtained for quadruple multiplexing was low. While transformation for single deletion resulted in ca. 200 transformants per plate, in identical conditions transformations with quadruple arrays yielded a 20-fold lower number of transformants. The low number of colonies obtained and tested did not allow to draw conclusions on a potential impact of *Fn*Cpf1 expression level on genome editing efficiency.

DISCUSSION

In the present study, *Fn*Cpf1 expressed as single copy from the *SGA1* locus using the strong and constitutive *TEF1*p promoter did not affect yeast physiology. Using the same cloning and expression strategy, Cas9 expression was similarly found to be neutral towards yeast growth (9). Conversely, higher expression levels of *Fn*Cpf1, mediated by expression from a multicopy plasmid, substantially impaired growth of *S. cerevisiae*, as previously reported for Cas9 (53,54). Generally, a stable integrated copy of Cpf1 is preferred, since this allows growth of strains on complex media and, when multiple rounds of transformation are required, efficient recycling of crRNA carrying plasmids.

Guided by earlier work performed *in vitro* and *in vivo*, the initial design of the crRNAs used in this study was based on a 5′-TTN-3′ PAM, a spacer of 25 nucleotides and direct repeats of 36 nucleotides (25,27,55). This design led to genome editing in *S. cerevisiae* with maximum efficiencies around 40%. Most influential for genome editing was the size reduction of the direct repeats from 36 to 19 nucleotides, as previously shown in mammalian cells (52), which consistently resulted in efficiencies of 100% for several targeted sites. The present work also demonstrated that *Fn*Cpf1 can be used for single nucleotide mutagenesis. While several studies reported that *Fn*Cpf1 is less efficient or even inactive for genome editing as compared to its orthologues *As*Cpf1 and *Lb*Cpf1 (for instance in rice (56), or in human cells (27,57)), the present study demonstrated that Cpf1 from *Francisella novicida* could efficiently and precisely cleave *S. cerevisiae* genome, thereby promoting homology directed repair.

A surprising outcome of this work was the clear and strong preference of *Fn*Cpf1 for crRNAs with 5′-TTTV-3′ as PAM, and without thymidine as first base after the PAM, when expressed in *S. cerevisiae*. These preferences are shared with its close relative *As*Cpf1 and *Lb*Cpf1. Structural studies of Cpf1 variants showed that the PAM duplex is bound to a groove formed by the WED, REC1, and PI domains (28,30). In this groove, the PAM duplex is recognized by Cpf1 by a combination of interactions with specific amino acids and by shape readout mechanisms (28,30). *Fn*Cpf1, *Lb*Cpf1 and *As*Cpf1 are remarkably well conserved in this region, and all amino acids suggested to be important for the 5′-TTTV-3′ PAM recognition by *As*Cpf1 are conserved in *Fn*Cpf1 (28,30,31). Also, a recent study on engineering *As*Cpf1 PAM specificity identified key amino acid residues that are also conserved in *Fn*Cpf1 (58). The high homology between F*n*Cpf1 and its orthologs suggested that it might also favour a 5′-TTTV-3′ PAM. Because editing of human cells by *Fn*Cpf1 initially was reported to be relatively inefficient (27), only a few studies reported its application for genome editing. In many of these studies the PAM sequence was fortuitously preceded by a thymidine. For instance, in the study by Fonfara *et al.*, in which the *Fn*Cpf1 PAM was relaxed from 5′-TTN-3′ to 5′-YTN-3′, the plasmid used to evaluate the PAM preference *in vivo* carried a thymidine located 5′ to the PAM (25). High throughput studies also suggest a slight preference for a thymidine preceding the 5′-YTN-3′ PAM for *Fn*Cpf1 (27,55). Altogether these observations seem to support the 5′-TTTV-3′ PAM preference found for *Fn*Cpf1 in the present study. This hypothesis should be further explored by a more systematic study of the PAM requirement for *Fn*Cpf1 in *S. cerevisiae*.

Based on the present results we recommend to apply the following criteria for crRNA design for Cpf1-based editing: (i) 5′-TTTV-3′ PAM, (ii) no thymidine in the first position of the crRNA spacer sequence, (iii) AT content between 30% and 70%, (iv) direct repeats of 19 nucleotides. Still, two crRNAs with optimal PAM and first position of the crRNA sequence (TTTA(C) for crADE2–4 and TTTC(A) for CAN1–2) did not lead to genome editing. As already observed for Cas9, other factors can also influence the efficiency of CRISPR endonuclease such as the presence of proteins or genomic DNA secondary structures that pre-

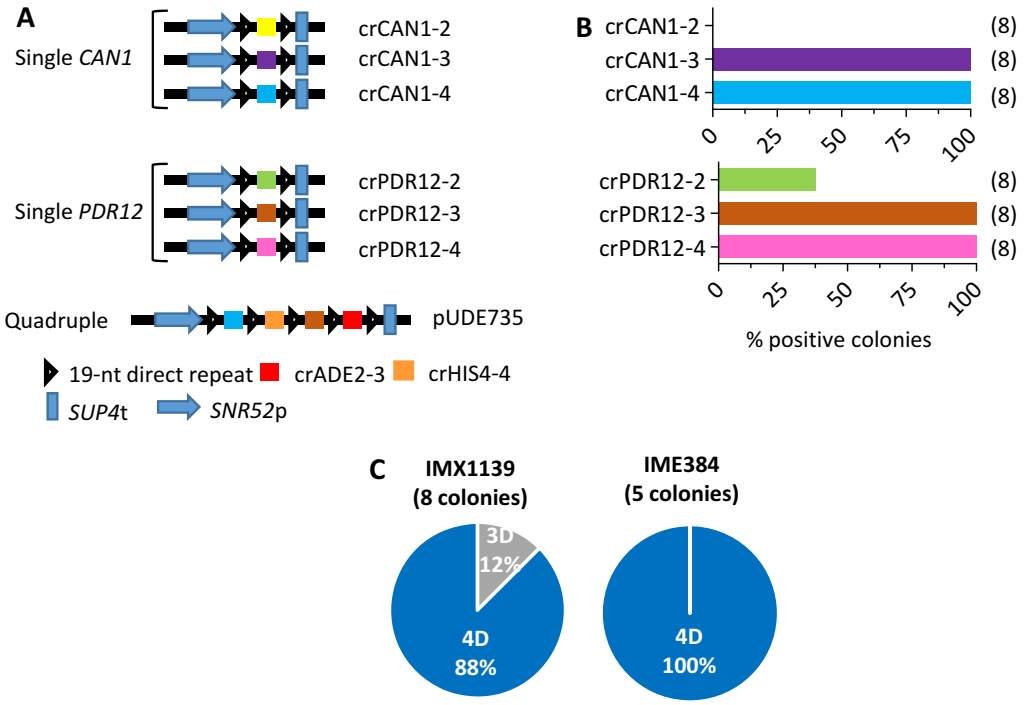

Figure 7. Multiplex genome editing by *Fn*Cpf1 in *S. cerevisiae*. (**A**) composition of CRISPR arrays for single deletion of *CAN1* and *PDR12*, and quadruple deletion of *ADE2*, *CAN1*, *HIS4*, and *PDR12*. Three different crRNAs were tested for *CAN1* and *PDR12*. 19-nt direct repeats were used and CRISPR plasmids were assembled *in vitro* using Gibson assembly. (**B**) Fraction of transformants with single deletion using single arrays (plasmids used: pUDE720 to pUDE725). (**C**) Fraction of clones with triple (3D) and quadruple deletion (4D) after transformation with the quadruple array (pUDE735). No transformants without deletion, or with single or double deletion were found. Two strains were tested for multiplex genome editing, IMX1139 with genomic integration of *Fncpf1* and IME384 in which *Fncpf1* is carried by a multicopy plasmid. B, C: deletion was quantified by diagnostic PCR (Supplementary Figure S6). The number of transformants checked by PCR is indicated between brackets. Plating was performed just after transformation, without additional incubation.

vent access of the endonuclease to the targeted genomic locus.

While using Cpf1 for single locus targeting already offers substantial advantages, such as the possibility to target AT-rich regions or to combine Cpf1 with other CRISPR-Cas enzymes such as Cas9, its major strength resides in its potential to edit the crRNA array itself, combined with the simplicity and short size of the crRNA array. In *S. cerevisiae*, applications of Cas9 for multisite editing remains rather limited, either because of the need of complicated DNA constructs in the case of a chimeric guide RNA, or because of low efficiency when CRISPR arrays are used (9,19,53,59,60). While ribozymes can compensate for the absence of crRNA cleavage by Cas9 in various organisms (61), their efficiency for multiplex genome editing has not been explored in *S. cerevisiae* yet. Furthermore, crRNA arrays equipped with ribozymes require complex DNA assembly or expensive custom DNA synthesis, as each expression unit, composed of two different ribozymes (typically Hammer Head and HDV) and of a single guide RNA, is 211 nt long (61). While 844 bp crRNA arrays are required to target four genes with artificial ribozyme and single guide RNA constructs using Cas9, simple, native 176 nt arrays suffice to promote quadruple genomic locus editing with *Fn*Cpf1 with 100% efficiency. *Fn*Cpf1 genome editing efficiency was not affected by the position of the crRNA on the array or by the number of protospacers when using up to four targets. The number of colonies obtained with quadruple crRNA arrays was strongly decreased as compared to single or double arrays. Overexpressing *Fn*Cpf1 using a multicopy plasmid did not increase the number of colonies obtained after transformation, suggesting that *Fn*Cpf1 was not a limiting factor for genome editing. This decrease in number of transformants can be explained by several factors, such as the decreased probability of the occurrence of multisite DNA cuts and repairs with increasing number of targets. In view of the absence of detectable benefit of expressing *Fn*Cpf1 from a multicopy plasmid for single or multisite editing up to four targets and of the toxicity of overexpression of *Fn*Cpf1, we advise to use single copy genomic integration of *Fncpf1* for genome editing in *S. cerevisiae*. Despite the low number of transformants obtained with multiplexing, which can be experimentally addressed, genome editing with *Fn*Cpf1 was remarkably efficient.

In conclusion, *Fn*Cpf1 is a powerful addition to the CRISPR toolbox in *S. cerevisiae*. The plasmid carrying *Fncpf1* framed by the *TEF1* promoter and *CYC1* terminator, as well as the plasmids expressing crRNAs for single and quadruple targeting of *ADE2*, *CAN1*, *HIS4* and *PDR12*, as well as double *ADE2* and *HIS4* targeting are available, and can be obtained through Addgene. Furthermore the tools supplied in this study provide an experimental foundation to easily express any crRNA. Cloning in pUD628 of 176 nt dsDNA fragment obtained by annealing

of two long oligonucleotides allows the facile construction of crRNA arrays of up to four spacer sequences and expands the application of *Fn*Cpf1 for editing the entire yeast genome.

SUPPLEMENTARY DATA

Supplementary Data are available at NAR online.

ACKNOWLEDGEMENTS

We thank Pilar de la Torre for sequencing IMX1139, Marcel van den Broek for bioinformatics support for whole genome sequence analysis and Mark Bisschops for critically reading the manuscript.

FUNDING

AdLibYeast ERC consolidator [648141 to P.D.L.]; European Union's Horizon 2020 Framework Programme for Research and Innovation; project: Model-Based Construction and Optimisation of Versatile Chassis Yeast Strains for Production of Valuable Lipid and Aromatic Compounds [720824 to J.M.D.]. Funding for open access charge: ERC consolidator [648141].
Conflict of interest statement. None declared.

REFERENCES

1. Barrangou,R., Fremaux,C., Deveau,H., Richards,M., Boyaval,P., Moineau,S., Romero,D.A. and Horvath,P. (2007) CRISPR provides acquired resistance against viruses in prokaryotes. *Science*, **315**, 1709–1712.
2. Jinek,M., Chylinski,K., Fonfara,I., Hauer,M., Doudna,J.A. and Charpentier,E. (2012) A programmable dual-RNA-guided DNA endonuclease in adaptive bacterial immunity. *Science*, **337**, 816–821.
3. van der Oost,J. (2013) Molecular biology. New tool for genome surgery. *Science*, **339**, 768–770.
4. Hsu,P.D., Lander,E.S. and Zhang,F. (2014) Development and applications of CRISPR-Cas9 for genome engineering. *Cell*, **157**, 1262–1278.
5. Estrela,R. and Cate,J.H. (2016) Energy biotechnology in the CRISPR-Cas9 era. *Curr. Opin. Biotechnol.*, **38**, 79–84.
6. Vervoort,Y., Linares,A.G., Roncoroni,M., Liu,C., Steensels,J. and Verstrepen,K.J. (2017) High-throughput system-wide engineering and screening for microbial biotechnology. *Curr. Opin. Biotechnol.*, **46**, 120–125.
7. Lee,J.H. and Wendisch,V.F. (2017) Production of amino acids—genetic and metabolic engineering approaches. *Bioresour. Technol.*, **245**,1575-1587.
8. DiCarlo,J.E., Norville,J.E., Mali,P., Rios,X., Aach,J. and Church,G.M. (2013) Genome engineering in *Saccharomyces cerevisiae* using CRISPR-Cas systems. *Nucleic Acids Res.*, **41**, 4336–4343.
9. Mans,R., van Rossum,H.M., Wijsman,M., Backx,A., Kuijpers,N.G., van den Broek,M., Daran-Lapujade,P., Pronk,J.T., van Maris,A.J. and Daran,J.M. (2015) CRISPR/Cas9: a molecular Swiss army knife for simultaneous introduction of multiple genetic modifications in *Saccharomyces cerevisiae*. *FEMS Yeast Res.*, **15**, fov004.
10. Lee,M.E., DeLoache,W.C., Cervantes,B. and Dueber,J.E. (2015) A highly characterized yeast toolkit for modular, multipart assembly. *ACS Synth. Biol.*, **4**, 975–986.
11. Makarova,K.S., Wolf,Y.I., Alkhnbashi,O.S., Costa,F., Shah,S.A., Saunders,S.J., Barrangou,R., Brouns,S.J., Charpentier,E., Haft,D.H. *et al.* (2015) An updated evolutionary classification of CRISPR-Cas systems. *Nat. Rev. Microbiol.*, **13**, 722–736.
12. Shmakov,S., Smargon,A., Scott,D., Cox,D., Pyzocha,N., Yan,W., Abudayyeh,O.O., Gootenberg,J.S., Makarova,K.S., Wolf,Y.I. *et al.* (2017) Diversity and evolution of class 2 CRISPR-Cas systems. *Nat. Rev. Microbiol.*, **15**, 169–182.
13. Mohanraju,P., Makarova,K.S., Zetsche,B., Zhang,F., Koonin,E.V. and van der Oost,J. (2016) Diverse evolutionary roots and mechanistic variations of the CRISPR-Cas systems. *Science*, **353**, aad5147.
14. Deltcheva,E., Chylinski,K., Sharma,C.M., Gonzales,K., Chao,Y., Pirzada,Z.A., Eckert,M.R., Vogel,J. and Charpentier,E. (2011) CRISPR RNA maturation by trans-encoded small RNA and host factor RNase III. *Nature*, **471**, 602–607.
15. van der Oost,J. (2015) Beat their swords into ploughshares. *Microb. Biotechnol.*, **8**, 34–35.
16. Deveau,H., Barrangou,R., Garneau,J.E., Labonte,J., Fremaux,C., Boyaval,P., Romero,D.A., Horvath,P. and Moineau,S. (2008) Phage response to CRISPR-encoded resistance in *Streptococcus thermophilus*. *J. Bacteriol.*, **190**, 1390–1400.
17. Bolotin,A., Quinquis,B., Sorokin,A. and Ehrlich,S.D. (2005) Clustered regularly interspaced short palindrome repeats (CRISPRs) have spacers of extrachromosomal origin. *Microbiology*, **151**, 2551–2561.
18. Mojica,F.J., Diez-Villasenor,C., Garcia-Martinez,J. and Almendros,C. (2009) Short motif sequences determine the targets of the prokaryotic CRISPR defence system. *Microbiology*, **155**, 733–740.
19. Bao,Z., Xiao,H., Liang,J., Zhang,L., Xiong,X., Sun,N., Si,T. and Zhao,H. (2015) Homology-integrated CRISPR-Cas (HI-CRISPR) system for one-step multigene disruption in *Saccharomyces cerevisiae*. *ACS Synth. Biol.*, **4**, 585–594.
20. Deaner,M., Mejia,J. and Alper,H.S. (2017) Enabling graded and large-scale multiplex of desired genes using a dual-mode dCas9 activator in *Saccharomyces cerevisiae*. *ACS Synth Biol.*, **6**, 1931-1943.
21. Zetsche,B., Gootenberg,J.S., Abudayyeh,O.O., Slaymaker,I.M., Makarova,K.S., Essletzbichler,P., Volz,S.E., Joung,J., van der Oost,J., Regev,A. *et al.* (2015) Cpf1 is a single RNA-guided endonuclease of a class 2 CRISPR-Cas system. *Cell*, **163**, 759–771.
22. Jiang,Y., Qian,F., Yang,J., Liu,Y., Dong,F., Xu,C., Sun,B., Chen,B., Xu,X., Li,Y. *et al.* (2017) CRISPR-Cpf1 assisted genome editing of *Corynebacterium glutamicum*. *Nat. Commun.*, **8**, 15179.
23. Kim,Y., Cheong,S.A., Lee,J.G., Lee,S.W., Lee,M.S., Baek,I.J. and Sung,Y.H. (2016) Generation of knockout mice by Cpf1-mediated gene targeting. *Nat. Biotechnol.*, **34**, 808–810.
24. Hur,J.K., Kim,K., Been,K.W., Baek,G., Ye,S., Hur,J.W., Ryu,S.M., Lee,Y.S. and Kim,J.S. (2016) Targeted mutagenesis in mice by electroporation of Cpf1 ribonucleoproteins. *Nat. Biotechnol.*, **34**, 807–808.
25. Fonfara,I., Richter,H., Bratovic,M., Le Rhun,A. and Charpentier,E. (2016) The CRISPR-associated DNA-cleaving enzyme Cpf1 also processes precursor CRISPR RNA. *Nature*, **532**, 517–521.
26. Endo,A., Masafumi,M., Kaya,H. and Toki,S. (2016) Efficient targeted mutagenesis of rice and tobacco genomes using Cpf1 from Francisella novicida. *Sci. Rep.*, **6**, 38169.
27. Zetsche,B., Gootenberg,J.S., Abudayyeh,O.O., Slaymaker,I.M., Makarova,K.S., Essletzbichler,P., Volz,S.E., Joung,J., van der Oost,J., Regev,A. *et al.* (2015) Cpf1 is a single RNA-guided endonuclease of a class 2 CRISPR-Cas system. *Cell*, **163**, 759–771.
28. Yamano,T., Nishimasu,H., Zetsche,B., Hirano,H., Slaymaker,I.M., Li,Y., Fedorova,I., Nakane,T., Makarova,K.S., Koonin,E.V. *et al.* (2016) Crystal structure of Cpf1 in complex with guide RNA and target DNA. *Cell*, **165**, 949–962.
29. Dong,D., Ren,K., Qiu,X., Zheng,J., Guo,M., Guan,X., Liu,H., Li,N., Zhang,B., Yang,D. *et al.* (2016) The crystal structure of Cpf1 in complex with CRISPR RNA. *Nature*, **532**, 522–526.
30. Stella,S., Alcon,P. and Montoya,G. (2017) Structure of the Cpf1 endonuclease R-loop complex after target DNA cleavage. *Nature*, **546**, 559–563.
31. Swarts,D.C., van der Oost,J. and Jinek,M. (2017) Structural basis for guide RNA processing and seed-dependent DNA targeting by CRISPR-Cas12a. *Mol. Cell*, **66**, 221–233.
32. Kim,H.K., Song,M., Lee,J., Menon,A.V., Jung,S., Kang,Y.M., Choi,J.W., Woo,E., Koh,H.C., Nam,J.W. *et al.* (2017) In vivo high-throughput profiling of CRISPR-Cpf1 activity. *Nat. Methods*, **14**, 153–159.
33. Fontana,L., Partridge,L. and Longo,V.D. (2010) Extending healthy life span–from yeast to humans. *Science*, **328**, 321–326.
34. Entian,K.D. and Kötter,P. (2007) In: Stansfield,I and Stark,MJR (eds). *Yeast Gene Analysis*. 2nd edn. Academic Press, Elsevier, Amsterdam, Vol. **36**, pp. 629–666.

35. Nijkamp,J.F., van den Broek,M., Datema,E., de,K.S., Bosman,L., Luttik,M.A., Daran-Lapujade,P., Vongsangnak,W., Nielsen,J., Heijne,W.H. *et al.* (2012) *De novo* sequencing, assembly and analysis of the genome of the laboratory strain *Saccharomyces cerevisiae* CEN.PK113-7D, a model for modern industrial biotechnology. *Microb. Cell Factor.*, doi:10.1186/1475-2859-11-36.
36. Verduyn,C., Postma,E., Scheffers,W.A. and van Dijken,J.P. (1992) Effect of benzoic acid on metabolic fluxes in yeasts: a continuous-culture study on the regulation of respiration and alcoholic fermentation. *Yeast*, **8**, 501–517.
37. Pronk,J.T. (2002) Auxotrophic yeast strains in fundamental and applied research. *Appl. Environ. Microbiol.*, **68**, 2095–2100.
38. Gietz,R.D. and Schiestl,R.H. (2007) Quick and easy yeast transformation using the LiAc/SS carrier DNA/PEG method. *Nat. Protoc.*, **2**, 35–37.
39. Looke,M., Kristjuhan,K. and Kristjuhan,A. (2011) Extraction of genomic DNA from yeasts for PCR-based applications. *Biotechniques*, **50**, 325–328.
40. Braglia,P., Percudani,R. and Dieci,G. (2005) Sequence context effects on oligo(dT) termination signal recognition by *Saccharomyces cerevisiae* RNA polymerase III. *J. Biol. Chem.*, **280**, 19551–19562.
41. Coordinators,N.R. (2013) Database resources of the National Center for Biotechnology Information. *Nucleic Acids Res.*, **41**, D8–D20.
42. Lorenz,R., Bernhart,S.H., Honer Zu Siederdissen,C., Tafer,H., Flamm,C., Stadler,P.F. and Hofacker,I.L. (2011) ViennaRNA Package 2.0. *Algorithms Mol. Biol.*, **6**, 26.
43. Kuijpers,N.G., Solis-Escalante,D., Bosman,L., van den Broek,M., Pronk,J.T., Daran,J.M. and Daran-Lapujade,P. (2013) A versatile, efficient strategy for assembly of multi-fragment expression vectors in *Saccharomyces cerevisiae* using 60 bp synthetic recombination sequences. *Microb. Cell Fact.*, **12**, 47.
44. Kuijpers,N.G., Chroumpi,S., Vos,T., Solis-Escalante,D., Bosman,L., Pronk,J.T., Daran,J.M. and Daran-Lapujade,P. (2013) One-step assembly and targeted integration of multigene constructs assisted by the I-SceI meganuclease in *Saccharomyces cerevisiae*. *FEMS Yeast Res.*, **13**, 769–781.
45. Li,H. and Durbin,R. (2010) Fast and accurate long-read alignment with Burrows-Wheeler transform. *Bioinformatics*, **26**, 589–595.
46. Li,H., Handsaker,B., Wysoker,A., Fennell,T., Ruan,J., Homer,N., Marth,G., Abecasis,G., Durbin,R. and Genome Project Data Processing, S. (2009) The Sequence Alignment/Map format and SAMtools. *Bioinformatics*, **25**, 2078–2079.
47. Dorfman,B.Z. (1969) The isolation of adenylosuccinate synthetase mutants in yeast by selection for constitutive behavior in pigmented strains. *Genetics*, **61**, 377–389.
48. Jakociunas,T., Bonde,I., Herrgard,M., Harrison,S.J., Kristensen,M., Pedersen,L.E., Jensen,M.K. and Keasling,J.D. (2015) Multiplex metabolic pathway engineering using CRISPR/Cas9 in *Saccharomyces cerevisiae*. *Metab. Eng.*, **28**, 213–222.
49. Ronda,C., Pedersen,L.E., Hansen,H.G., Kallehauge,T.B., Betenbaugh,M.J., Nielsen,A.T. and Kildegaard,H.F. (2014) Accelerating genome editing in CHO cells using CRISPR Cas9 and CRISPy, a web-based target finding tool. *Biotechnol. Bioeng.*, **111**, 1604–1616.
50. Labun,K., Montague,T.G., Gagnon,J.A., Thyme,S.B. and Valen,E. (2016) CHOPCHOP v2: a web tool for the next generation of CRISPR genome engineering. *Nucleic Acids Res.*, **44**, W272–W276.
51. Wang,T., Wei,J.J., Sabatini,D.M. and Lander,E.S. (2014) Genetic screens in human cells using the CRISPR-Cas9 system. *Science*, **343**, 80–84.
52. Zetsche,B., Heidenreich,M., Mohanraju,P., Fedorova,I., Kneppers,J., DeGennaro,E.M., Winblad,N., Choudhury,S.R., Abudayyeh,O.O., Gootenberg,J.S. *et al.* (2017) Multiplex gene editing by CRISPR-Cpf1 using a single crRNA array. *Nat. Biotechnol.*, **35**, 31–34.
53. Ryan,O.W., Skerker,J.M., Maurer,M.J., Li,X., Tsai,J.C., Poddar,S., Lee,M.E., DeLoache,W., Dueber,J.E., Arkin,A.P. *et al.* (2014) Selection of chromosomal DNA libraries using a multiplex CRISPR system. *Elife*, **3**, doi:10.7554/eLife.03703.
54. Generoso,W.C., Gottardi,M., Oreb,M. and Boles,E. (2016) Simplified CRISPR-Cas genome editing for *Saccharomyces cerevisiae*. *J. Microb. Methods*, **127**, 203–205.
55. Leenay,R.T., Maksimchuk,K.R., Slotkowski,R.A., Agrawal,R.N., Gomaa,A.A., Briner,A.E., Barrangou,R. and Beisel,C.L. (2016) Identifying and visualizing functional PAM diversity across CRISPR-Cas systems. *Mol. Cell*, **62**, 137–147.
56. Wang,M., Mao,Y., Lu,Y., Tao,X. and Zhu,J.K. (2017) Multiplex gene editing in rice using the CRISPR-Cpf1 system. *Mol. Plant*, **10**, 1011-1013.
57. Kim,D., Kim,J., Hur,J.K., Been,K.W., Yoon,S.H. and Kim,J.S. (2016) Genome-wide analysis reveals specificities of Cpf1 endonucleases in human cells. *Nat. Biotechnol.*, **34**, 863–868.
58. Gao,L., Cox,D.B.T., Yan,W.X., Manteiga,J.C., Schneider,M.W., Yamano,T., Nishimasu,H., Nureki,O., Crosetto,N. and Zhang,F. (2017) Engineered Cpf1 variants with altered PAM specificities. *Nat.Biotechnol.*, **35**, 789-792.
59. Horwitz,A.A., Walter,J.M., Schubert,M.G., Kung,S.H., Hawkins,K., Platt,D.M., Hernday,A.D., Mahatdejkul-Meadows,T., Szeto,W., Chandran,S.S. *et al.* (2015) Efficient multiplexed integration of synergistic alleles and metabolic pathways in yeasts via CRISPR-Cas. *Cell Syst.*, **1**, 88–96.
60. Wong,A.S., Choi,G.C., Cui,C.H., Pregernig,G., Milani,P., Adam,M., Perli,S.D., Kazer,S.W., Gaillard,A., Hermann,M. *et al.* (2016) Multiplexed barcoded CRISPR-Cas9 screening enabled by CombiGEM. *Proc. Natl. Acad. Sci. U.S.A.*, **113**, 2544–2549.
61. Gao,Y. and Zhao,Y. (2014) Self-processing of ribozyme-flanked RNAs into guide RNAs *in vitro* and *in vivo* for CRISPR-mediated genome editing. *J. Integr. Plant Biol.*, **56**, 343–349.
62. Sikorski,R.S. and Hieter,P. (1989) A system of shuttle vectors and yeast host strains designed for efficient manipulation of DNA in *Saccharomyces cerevisiae*. *Genetics*, **122**, 19–27.